Acta Scientific CANCER BIOLOGY (ISSN: 2582-4473)

Volume 9 Issue 1 January 2025

Research Article

Structural Analysis, Topological Studies and Biological Evaluation on N-hydroxymethyl Phthalimide - an Insight into Anticancer Activity

Dona Benny[1], A Anuradha[2] and Johanan Christian Prasana[1]*

[1]Department of Physics, Madras Christian College, East Tambaram, University of Madras, Chennai, Tamilnadu, India

[2]PG and Research Department of Physics, Queen Mary's College(A), Chennai-600 004,

***Corresponding Author:** Johanan Christian Prasana, Department of Physics, Madras Christian College, East Tambaram, Chennai, Tamilnadu, India.

Received: March 28, 2025

Published: April 29, 2025

Abstract

Phthalimide derivatives are a versatile scaffold for designing novel drug candidates and have shown promise in treating a variety of diseases, including cancer. Cancer remains a devastating disease, demanding continued research and improved treatment strategies due to its severe adverse effects. This study employs computational and experimental techniques to investigate the properties and potential biological activity of N-hydroxymethyl phthalimide. DFT calculations, using B3LYP (functional) with a basis set, 6311++G(d,p), were utilized in Structural analysis, Topological studies, and Biological evaluation. Molecular geometry and FT-IR and FT-Raman spectroscopy were employed to characterize the structural properties of compound. Topological analysis (MEP, ELF, LOL) was performed. To assess potential biological activity of N-hydroxymethyl phthalimide, UV-Vis analysis, FMO analysis, drug-likeness, and molecular docking studies were conducted. *In vitro*, cytotoxicity assays were also performed to evaluate the compound's cytotoxic effect on human skin melanoma cell-line. Results predict that N-hydroxymethyl phthalimide exhibits anti-cancer activity, indicating its potential as a promising agent for inhibiting cancer.

Keywords: Phthalimides; Drug-Likeness Properties; *In Vitro* Assay Studies; Molecular Docking; Anti-Cancer Activity; Skin Melanoma

Introduction

Phthalimides, a class of bicyclic non-aromatic nitrogen heterocycles, offer a wide range of applications. Phthalimide-containing compounds as a versatile scaffold for designing novel drug candidates. These compounds have shown promise in treating a variety of diseases, including cancer, diabetes, multiple myeloma, seizures, inflammation, pain, and bacterial infections [1,2]. It is a versatile pharmacophore with a broad spectrum of biological activities and a key component in medicinal chemistry [3]. Thalidomide, a drug containing a phthalimide ring, is used to treat epilepsy and has immunomodulatory properties [4]. Phthalimide analogs have attracted significant scientific interest due to their potent ability to inhibit various cancer-causing receptors [5,6]. Cancer remains a devastating disease, demanding continued research and improved treatment strategies due to its severe adverse effects.

Phthalimide derivatives have substantial interest due to their diverse applications. This study centers on N-Hydroxymethyl phthalimide ($C_9H_7NO_3$), with a molecular weight of 177.16 g/mol, which is not been previously investigated using DFT. To explore the potential applications and properties of this compound, a comprehensive analysis was conducted. DFT studies were performed to elucidate molecular structure of N-hydroxymethyl phthalimide. To assess the compound's biological potential and pharmaceutical relevance, biological studies were conducted. A standard drug with the same biological activity was chosen and results obtained in biological studies were compared in understanding the potential of the title compound.

Experimental details

N-Hydroxymethyl phthalimide (purity > 98%) was procured from Tokyo Chemical Industry Co., Ltd. FT-IR spectrum was recorded on a KBr pellet (4000-400 cm^{-1} range). FT-Raman spectrum was obtained (range 4000-100 cm^{-1}). All spectroscopic measurements were performed at the Sophisticated Analytical Instrumentation Facility (SAIF), IIT Madras. *In vitro* cytotoxicity studies of N-Hydroxymethyl phthalimide were conducted at Radiant Research Services Pvt. Ltd., Bengaluru, India.

Computational details

For all DFT calculations, Gaussian 16W [7,8] software packages were utilized. B3LYP is the functional and 6-311G++(d,p) is the basis set employed. Vibrational assignments were obtained using Veda software [9] Surface analysis, including MEP, ELF, and LOL, was performed using Multiwfn 3.8 [10]. Drug-likeness properties were assessed using SwissADME [11] online tool. PASS online tool [12] was utilized to predict potential bioactivity of N-hydroxymethyl phthalimide. AutoDockTools 1.5.6 [13] was the software used in molecular docking simulations. The resulting protein-ligand complexes were visualized using Discovery Studio [14].

Results and Discussion

Structural analysis

Molecular geometry is the 3-dimensional spatial arrangement of atoms within a molecule determined by the bond parameters.

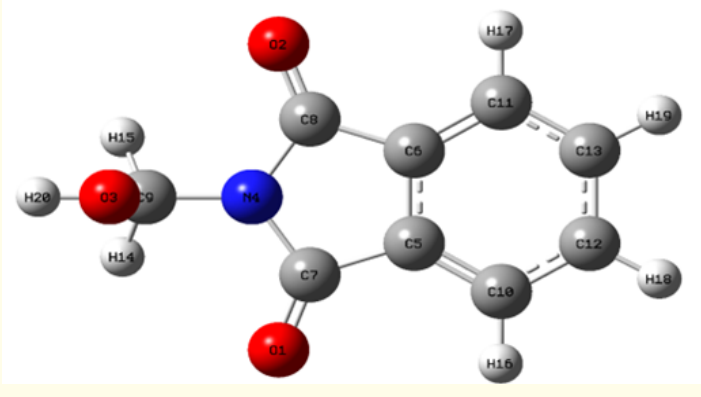

Figure 1: Optimized molecular geometry of N-Hydroxymethyl phthalimide.

Optimized structure is the most stable structure obtained using DFT calculations and Fig. 1. is the optimized structure of N-Hydroxymethyl phthalimide. Bond parameters are given in table 1. In the C6-C8 bond, Carbon atom(C8) is also bonded with more electronegative oxygen (O2) and the nitrogen atom(N4) resulting in a longer bond length (1.463 Å). Carbon-carbon bonds within the rings are found to be higher and almost equal. High Electronegativity of oxygen atom and strong covalent bond between oxygen and hydrogen atoms might be responsible for the shortest bond between O3-H20 (0.972 Å) atoms.\

Bond length between Carbon atoms (C7, C8) and oxygen atoms (O1, O2) was found to be 1.217 Å and the bond length between O3-C9 was 1.415 Å. Higher bond order between O1-C7 and O2-C8 are responsible for the shorter bond length than the bond length of O3-C9 atoms indicating a higher bond strength. Bond lengths C9-H14 and C9-H15 are 1.094 Å, C10-H16 and C11-H17 are 1.084 Å, C12-H18 and C13-H19 are 1.087 Å. Carbon and hydrogen atoms show a shorter and nearly equal bond length due to a strong covalent bond. Largest bond angle was observed between O2-C8-N4 (130.4°), and the smallest bond angle between N4-C7-C5 and N4-C8-C6 (105.7°). Molecular geometry of N-hydroxymethyl phthalimide provided an insight into the structural analysis and biological activity of the molecule [15-18].

Atoms	Bond Length(Å)	Atoms	Bond Angle (°)
O1-C7	1.217	O1-C7-N4	130.1
O2-C8	1.217	O1-C7-C5	124.2
O3-C9	1.415	O2-C8-N4	130.4
O3-H20	0.972	O2-C8-C6	124
N4-C7	1.379	C9-O3-H20	107.1
N4-C8	1.379	O3-C9-N4	109
N4-C9	1.449	O3-C9-H14	108.9
C5-C6	1.387	O3-C9-H15	108.9
C5-C7	1.462	C7-N4-C8	112.6
C5-C10	1.38	C7-N4-C9	123.7
C6-C8	1.463	N4-C7-C5	105.7
C6-C11	1.38	C8-N4-C9	123.7
C9-H14	1.094	N4-C8-C6	105.7
C9-H15	1.094	N4-C9-H14	109.7
C10-C12	1.398	N4-C9-H15	109.7
C10-H16	1.084	C6-C5-C7	108.1
C11-C13	1.398	C6-C5-C10	121.9
C11-H17	1.084	C5-C6-C8	108.1
C12-C13	1.41	C5-C6-C11	122
C12-H18	1.087	C7-C5-C10	130
C13-H19	1.087	C5-C10-C12	117.1
		C5C-10-H16	122
		C8-C6-C11	130
		C6-C11-C13	117.1
		C6-C11-H17	122
		H14-C9-H15	110.6
		C12-C10-H16	120.9
		C10-C12-C13	120.9
		C10-C12-H18	119.7
		C13-C11-H17	120.9
		C11-C13-C12	120.9
		C11-C13-H19	119.7
		C13-C12-H18	119.4
		C12-C13-H19	119.4

Table 1: Bond parameters of N-hydroxymethyl phthalimide.

Vibrational analysis

Vibrational analysis is valuable in structure interpretation by studying functional groups within molecules. N-hydroxymethyl phthalimide exhibits 54 vibrational modes (3n-6). This study compares experimental FT-IR, and FT-Raman spectra with theoretical. A scaling factor of 0.961 is incorporated in theoretical calculations since the theoretical computations were done in gas phase. [19,20]. Theoretical and experimental spectra for both FT-IR and FT-Raman demonstrate excellent correlation, as shown in figure 2. Vibrational assignments are listed in Table 2. O-H stretching vibrations are observed 3600-3400 cm^{-1} range [21]. Pure O-H stretching peak was observed for title compound, since PED values are 100%, at 3692 cm^{-1} and 3684 cm^{-1} for experimental FT-IR and theoretical FT- IR respectively. C-H stretching vibrations typically occur within the range from 3000 to 3100 cm^{-1} [22] and the Experimental FT-IR

peak and FT-Raman peak for C-H stretching was observed at 3042 $cm^{-1}$and 3066 cm^{-1}, respectively. Theoretical peaks (3039 cm^{-1} and 3087 cm^{-1}) for C-H stretching was also observed within standard range. Also, from theoretical and experimental observation pure C-H stretching vibrations were identified at 2963 $cm^{-1}$and 2965 cm^{-1} for FT-IR and FT-Raman respectively. The desired region for C-O stretching is between 1740 and 1660 cm^{-1} [23] and the Experimental FT-IR and FT-Raman peaks were observed at 1770 cm^{-1} and 1769cm^{-1}, respectively. Theoretical peaks (1762 and 1714 cm^{-1}) for C-O vibrations were also fall within the desired range. C-C stretching vibrations typically occur from 1650 to1400 cm^{-1} [24] and the corresponding experimental FT-IR, experimental FT-Raman and theoretical peaks were observed at 1439 cm^{-1}, 1459 cm^{-1} and 1458 cm^{-1}, respectively. Experimental and theoretical vibrational spectroscopic data of the chosen compound are in line with each other.

Modes	Wavenumber(cm)								Assignments (PED)%
	Experimental		Theoretical		IR intensity		Raman activity		
	FT IR	FT Raman	unscaled	scaled*	Rel	abs**	Rel	abs**	
54	3692		3834	3684	42	6	239	86	ϒ OH(100)
53			3201	3076	8	1	278	100	ϒ CH(100)
52			3198	3073	3	0	27	10	ϒ CH(90)
51			3186	3062	5	1	123	44	ϒ CH(100)
50	3042	3066	3173	3050	2	0	60	22	ϒ CH(90)
49	2963	2965	3087	2966	7	1	51	18	ϒ CH(100)
48			3039	2920	40	6	115	41	ϒ CH(100)
47	1770	1769	1834	1762	106	15	126	45	ϒ OC(80)
46		1723	1783	1714	712	100	21	7	ϒ OC(88)
45			1647	1583	16	2	40	14	ϒ CC(72)
44			1643	1579	2	0	9	3	ϒ CC(31)+ βCCC(30)
43	1459	1458	1497	1439	19	3	14	5	βHCH(81)
42			1497	1438	6	1	2	1	ϒ CC(20)+ βHCC(60)
41	1425		1493	1435	3	0	1	0	ϒ CC(14)+βHCC(40)+βCCC(10)
40	1403	1408	1463	1405	2	0	4	1	βHOC(12)+βHCH(12)+τ HCNC(65)
39	1350	1353	1398	1343	492	69	40	14	ϒ NC(34)+βCNC(28)
38			1383	1329	8	1	2	1	ϒ CC(58)
37	1316		1353	1301	22	3	10	4	βHCO(56)+τ HCNC(28)
36			1310	1258	0	0	0	0	βHCC(46)
35	1199	1186	1244	1195	106	15	37	13	βHOC(52)
34		1159	1205	1158	33	5	34	12	ϒ CC(35)+βHOC(21)
33			1197	1150	38	5	2	1	ϒ NC(26)+βHCO(20)+βCNC(11)+τ HCNC(25)
32	1145		1190	1144	3	0	5	2	ϒ CC(24)+βCCC(12)+βHCC(20)+βCCC(12)
31			1180	1134	6	1	12	4	βHCC(66)
30	1052	1051	1100	1057	7	1	1	0	ϒ CC(20)+ βCCC(22)+βHCC(20)+βCCC(11)
29		1018	1044	1004	113	16	6	2	ϒ OC(67)
28			1033	993	14	2	39	14	ϒ OC(19)+βHCC(20)+βCCC(28)
27	976		1011	972	0	0	0	0	τ HCCC(23)+τ CCCC(65)
26			985	946	86	12	2	1	ϒ NC(41)+βHCO(14)+τ HCNC(15)
25			985	946	1	0	0	0	τ HCCC(92)
24			974	936	7	1	3	1	ϒ CC(20)+ϒ NC(31)
23			910	874	0	0	0	0	τ HCCC(86)
22	848		863	829	4	1	4	1	βCCC(28)+βNCC(14)
21			807	776	0	0	0	0	τ NCCC(15)+ωONCC(50)

20			807	776	12	2	1	0	τ HCCC(40)+ωCCCC(39)
19	708	713	739	710	64	9	2	1	τ HCCC(28)+ωCCCC(32)
18			721	693	13	2	18	7	ϒ CC(28)
17	670		706	679	2	0	0	0	βOCC(50)+βCCC(11)
16	665		683	657	0	0	0	0	τ CCCC(62)+ωONCC(23)
15			617	593	44	6	8	3	ϒ NC(11)+βCNC(39)+βOCN(13)
14	564	566	564	542	34	5	5	2	βOCN(13)
13	530		537	516	10	1	1	0	ϒ CC(24)+ϒ NC(13)+βCCC(11)+βNCC(17)
12			464	446	0	0	0	0	τ CCCC(70)
11			427	410	2	0	3	1	τ CCCC(24)
10		397	402	387	0	0	3	1	βOCN(14)+τ CCCC(30)
9			348	334	14	2	1	0	βOCC(50)
8		244	279	268	3	0	1	0	βCNC(50)
7			236	227	1	0	1	0	βCCC(57)+βCNC(16)
6			191	184	1	0	1	0	ωCCCN(16)+ωCCCC(57)
5		164	150	144	3	0	0	0	τ CNCC(62)+τ NCCC(14)
4			146	140	48	7	1	0	τ HOCN(29)+τ NCCC(22)+τ OCNC(17)
3		121	131	126	42	6	1	0	τ HOCN(26)+τ CCCC(14)+τ NCCC(31)
2			69	67	7	1	2	1	ωCCCN(67)+ωCCCC(18)
1			46	44	30	4	3	1	τ HOCN(45)+τ OCNC(40)

Table 2: Experimental and calculated vibrational spectroscopic data with vibrational assignments N-hydroxymethyl phthalimide.

Topological studies

Molecular electrostatic potential (MEP)

Fig.3. presents the MEP map for N-Hydroxymethyl phthalimide. MEP scale ranges from -5.440e^{-2} to +5.440e^{-2}. MEP map is a 3-dimensional surface analysis illustrating the distribution of electron density within a molecule. MEP maps the regions of high and low electron density and thus identifying nucleophilic and electrophilic attacking sites. Blue> Green> Yellow>Red is the decreasing order of electrostatic potential in MEP contour. According to color grading, nucleophilic attacking sites are represented in blue color while electrophilic attacking sites are represented in red region and the green region depicts zero potential on the map. In MEP, oxygen atoms (O1 and O2) attached to carbon atoms (C7 and C8) and O3 are located more toward the negative potential region suggest that it might be a site for electrophilic attack and blue region near hydrogen atom (H20) suggests the nucleophilic attack indicating possible interaction sites to enhanced the biological activity of the title compound. [25-27].

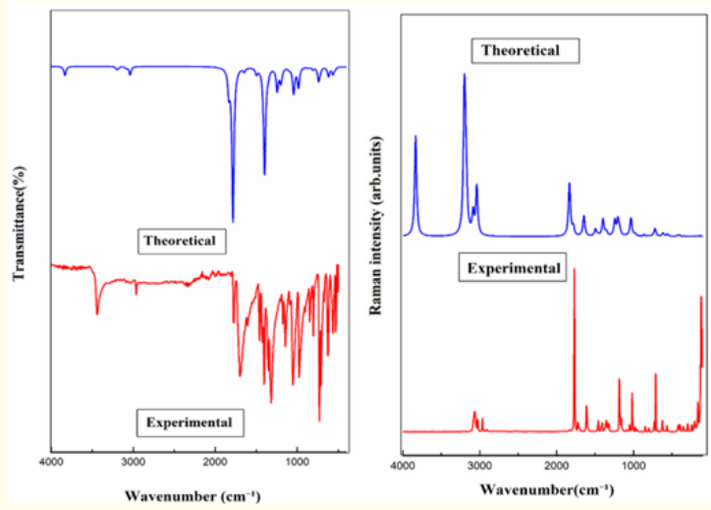

Figure 2: FT-IR and FT-Raman spectra.

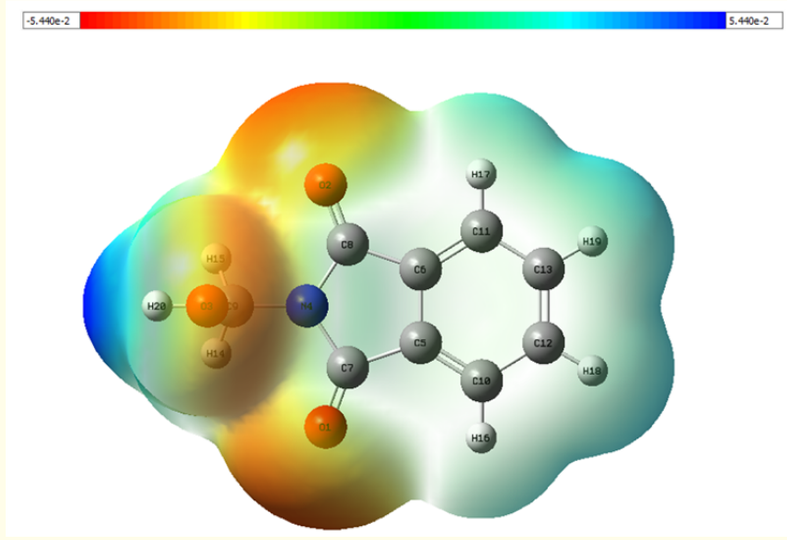

Figure 3: Molecular Electrostatic Potential map.

Electron localization function (ELF) and localized orbital locator (LOL).

ELF and LOL are contemporary tools employed to analyze the distribution of electron density within molecular systems. ELF and LOL colored maps are generated for N-Hydroxymethyl phthalimide using Mutiwfn 3.8 software and are presented in figure 4.

ELF employs a color-coded scale from deep blue to red having values ranging from 0 to 1.0 (Fig 4), where blue colour corresponds to minimal electron localization probability and red colour corresponds to maximal electron localization probability [28,29]. A value below 0.5 on the scale suggests low electron delocalization [30]. Hydrogen atoms (H16, H17, H18, H19) were seen in red region depicting maximum localization of electrons leading to maximum Pauli's repulsion [30] and Carbon atoms (C10, C11) were in blue region indicating minimum electron localization hence minimum Pauli's repulsion [30] indicating an interaction between carbon and hydrogen [refer Figure 1].

LOL visualizes localized orbitals [31] and its scale ranges from 0 to 0.8 indicated by deep blue to red. Blue represents regions of low electron localization, while red indicates regions of high electron localization [32]. H16, H17, H18, and H19 atoms were seen in the red region of LOL map indicating maximum electron localization [33] and C10 and C11 atoms are in blue region suggesting low electron localization [33] which compliments ELF studies. Thus, LOL and ELF complement each other.

Surface analysis (MEP, ELF, and LOL maps) predicts the possible chemical bonding and interactions, which might play a crucial role in understanding the biological activity of the title compound.

Natural bonding orbital (NBO) analysis

NBO analysis was conducted on the title compound to investigate conjugative interactions and charge transfer within the molecular system, leading to understand about the molecular stability, and the results are presented in Table 3. Electron interaction between donors and acceptors were analyzed using NBO and highest stabilization energy suggests the strong interaction. The highest stabilization energy of 188 kcal/mol is observed during the transition of electrons between O2-C8 (donor) and C6-C11 (acceptor), O1-C7 (donor) and C5-C10 (acceptor) which may be due to the electrophilic attack region over oxygen as indicated in MEP studies (ref fig 4). Other stabilization energies of 47.2 kcal/mol and 47.1 kcal/mol were found during the transition of electrons between N4 (acceptor) and O1-C7 (donor), and N4 (acceptor) and O2-C8 (donor), respectively [34,35]. Strong interaction between electron donor and electron acceptor was identified with the higher stabilization energy values and NBO analysis studied the contribution of hyper-conjugative interactions and charge delocalization to stability [36].

UV-Vis analysis

UV-Vis spectroscopy is a powerful analytical tool used to examine interaction of chemical substances with UV and visible light.

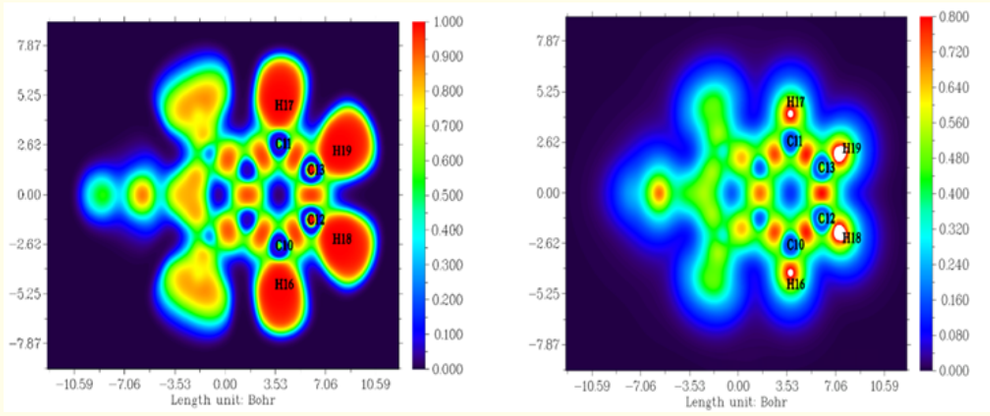

Figure 4: ELF and LOL map of N-hydroxymethyl phthalimide.

Donor	Type	ED/e (q_i)	Acceptor	Type	ED/e (q_i)	E(2)	E(j)-E(i)	F(i,j)
O 2 - C 8	π	0.228	C 6 - C 11	π*	0.337	188	0.01	0.076
O 1 - C 7	π	0.228	C 5 - C 10	π*	0.337	188	0.01	0.076
N 4	LP (1)	1.636	O 1 - C 7	π*	0.228	47.2	0.28	0.106
N 4	LP (1)	1.636	O 2 - C 8	π*	0.228	47.1	0.28	0.106
O 1	LP (2)	1.853	N 4 - C 7	σ*	0.095	29.8	0.66	0.127
O 2	LP (2)	1.853	N 4 - C 8	σ*	0.095	29.8	0.66	0.127
C 5 - C 10	π	1.634	C 6 - C 11	π*	0.337	21.1	0.29	0.07
C 6 - C 11	π	1.634	C 5 - C 10	π*	0.337	21.1	0.29	0.07
C 12 - C 13	π	1.639	C 5 - C 10	π*	0.337	19.8	0.29	0.068
C 12 - C 13	π	1.639	C 6 - C 11	π*	0.337	19.8	0.29	0.068
O 1	LP (2)	1.853	C 5 - C 7	σ*	0.071	19.5	0.69	0.105
O 2	LP (2)	1.853	C 6 - C 8	σ*	0.071	19.5	0.69	0.105
C 5 - C 10	π	1.634	C 12 - C 13	π*	0.311	19.2	0.28	0.067
C 6 - C 11	π	1.634	C 12 - C 13	π*	0.311	19.2	0.28	0.067
C 5 - C 10	π	1.634	O 1 - C 7	π*	0.228	17.5	0.28	0.065
C 6 - C 11	π	1.634	O 2 - C 8	π*	0.228	17.5	0.28	0.065
N 4	LP (1)	1.636	O 3 - C 9	σ*	0.032	11.9	0.54	0.078
O 3	LP (2)	1.96	C 9 - H 15	σ*	0.0266	6.25	0.69	0.059
O 3	LP (2)	1.96	C 9 - H 14	σ*	0.0266	6.23	0.69	0.059
C 5 - C 10	σ	1.976	C 5 - C 6	σ*	0.026	5.09	1.29	0.072
C 6 - C 11	σ	1.976	C 5 - C 6	σ*	0.026	5.09	1.29	0.072
C 10 - C 12	σ	1.987	C 5 - C 7	σ*	0.071	4.54	1.13	0.065
C 11 - C 13	σ	1.978	C 6 - C 8	σ*	0.071	4.54	1.13	0.065
C 5 - C 6	σ	1.964	C 5 - C 10	σ*	0.021	4.48	1.28	0.068
C 5 - C 6	σ	1.964	C 6 - C 11	σ*	0.021	4.48	1.28	0.068
C 10 - H 16	σ	1.979	C 5 - C 6	σ*	0.026	4.37	1.1	0.062
C 11 - H 17	σ	1.979	C 5 - C 6	σ*	0.026	4.37	1.1	0.062
C 5 - C 7	σ	1.971	C 6 - C 11	σ*	0.021	4.13	1.24	0.064
C 6 - C 8	σ	1.971	C 5 - C 10	σ*	0.021	4.13	1.24	0.064

C 5 - C 7	σ	1.971	N 4 - C 9	σ*	0.036	4.03	1.02	0.057
C 6 - C 8	σ	1.971	N 4 - C 9	σ*	0.036	4.03	1.02	0.057
O 1 - C 7	π	1.973	C 5 - C 10	π*	0.337	3.97	0.41	0.039
O 2 - C 8	π	1.973	C 6 - C 11	π*	0.337	3.97	0.41	0.039
C 12 - H 18	σ	1.98	C 11 - C 13	σ*	0.014	3.95	1.09	0.059
C 13 - H 19	σ	1.98	C 10 - C 12	σ*	0.014	3.95	1.09	0.059
C 9 - H 14	σ	1.987	N 4 - C 8	σ*	0.095	3.89	0.92	0.054
C 9 - H 15	σ	1.987	N 4 - C 7	σ*	0.095	3.89	0.92	0.054
C 10 - H 16	σ	1.979	C 12 - C 13	σ*	0.015	3.54	1.09	0.055
C 11 - H 17	σ	1.979	C 12 - C 13	σ*	0.015	3.54	1.09	0.055
C 5 - C 6	σ	1.964	O 1 - C 7	σ*	0.228	3.37	1.31	0.06
C 5 - C 6	σ	1.964	O 2 - C 8	σ*	0.01	3.37	1.31	0.06
C 12 - H 18	σ	1.98	C 5 - C 10	σ*	0.021	3.31	1.11	0.054
C 13 - H 19	σ	1.98	C 6 - C 11	σ*	0.021	3.31	1.11	0.054
O 3	LP (1)	1.978	N 4 - C 9	σ*	0.036	3.25	0.98	0.05
C 10 - C 12	σ	1.987	C 5 - C 10	σ*	0.021	3.17	1.29	0.057
C 11 - C 13	σ	1.978	C 6 - C 11	σ*	0.021	3.17	1.29	0.057
N 4 - C 7	σ	1.985	O 2 - C 8	σ*	0.01	2.96	1.4	0.058
N 4 - C 8	σ	1.985	O 1 - C 7	σ*	0.228	2.96	1.4	0.058
O 1	LP (1)	1.979	C 5 - C 7	σ*	0.071	2.54	1.11	0.048
O 2	LP (1)	1.979	C 6 - C 8	σ*	0.071	2.54	1.11	0.048
N 4 - C 8	σ	1.985	C 6 - C 11	σ*	0.021	2.51	1.37	0.052
N 4 - C 7	σ	1.985	C 5 - C 10	σ*	0.021	2.5	1.37	0.052
C 5 - C 10	σ	1.976	C 10 - C 12	σ*	0.014	2.46	1.28	0.05
C 6 - C 11	σ	1.976	C 11 - C 13	σ*	0.014	2.46	1.28	0.05
C 6 - C 11	σ	1.976	C 6 - C 8	σ*	0.071	2.45	1.14	0.048
C 5 - C 10	σ	1.976	C 5 - C 7	σ*	0.071	2.44	1.14	0.048
C 12 - C 13	σ	1.98	C 10 - C 12	σ*	0.014	2.42	1.27	0.05
C 12 - C 13	σ	1.98	C 11 - C 13	σ*	0.014	2.42	1.27	0.05
C 5 - C 6	σ	1.964	C 10 - H 16	σ*	0.013	2.37	1.14	0.047
C 5 - C 6	σ	1.964	C 11 - H 17	σ*	0.013	2.37	1.14	0.047
C 10 - C 12	σ	1.987	C 12 - C 13	σ*	0.015	2.37	1.27	0.049
C 11 - C 13	σ	1.978	C 12 - C 13	σ*	0.015	2.37	1.27	0.049
O 3 - H 20	σ	1.985	N 4 - C 9	σ*	0.036	2.32	1.07	0.045
C 12 - C 13	σ	1.98	C 10 - H 16	σ*	0.013	2.3	1.15	0.046
C 12 - C 13	σ	1.98	C 11 - H 17	σ*	0.013	2.3	1.15	0.046
C 5 - C 10	σ	1.976	C 12 - H 18	σ*	0.012	2.23	1.16	0.046
C 6 - C 11	σ	1.976	C 13 - H 19	σ*	0.012	2.23	1.16	0.046
C 5 - C 7	σ	1.971	C 5 - C 10	σ*	0.021	2.11	1.24	0.046
C 6 - C 8	σ	1.971	C 6 - C 11	σ*	0.021	2.11	1.24	0.046
O 1 - C 7	σ	1.994	C 5 - C 7	σ*	0.071	2.09	1.52	0.051
O 2 - C 8	σ	1.994	C 6 - C 8	σ*	0.071	2.09	1.52	0.051
C 10 - C 12	σ	1.987	C 13 - H 19	σ*	0.012	2.08	1.15	0.044
C 11 - C 13	σ	1.978	C 12 - H 18	σ*	0.012	2.08	1.15	0.044
C 5 - C 7	σ	1.971	O 1 - C 7	σ*	0.228	1.91	1.27	0.044

Table 3: Second-order perturbation theory analysis of Fock matrix in NBO basis N-hydroxymethyl phthalimide.

UV-Vis spectroscopy focuses from 200 to 800 nm region, where 10-400 nm is in the UV region and 400-780 nm in the visible region of Electro Magnetic spectrum [37, 38]. TD-DFT approach with B3LYP/ 6-311++G(d,p) basis set is employed to simulate theoretical UV visible spectra of N-hydroxymethyl phthalimide and Fig.5 shows theoretical UV-Vis spectrum and Table 4 shows the electronic properties of title compound. Absorption peak for the title compound was found to be at 286.46nm which is in the mid UV region of EM spectrum and thus, moderate amount of energy may be required to exciting an electron from lower occupied orbital to higher unoccupied orbital suggesting the moderate stability of the chosen compound [39].

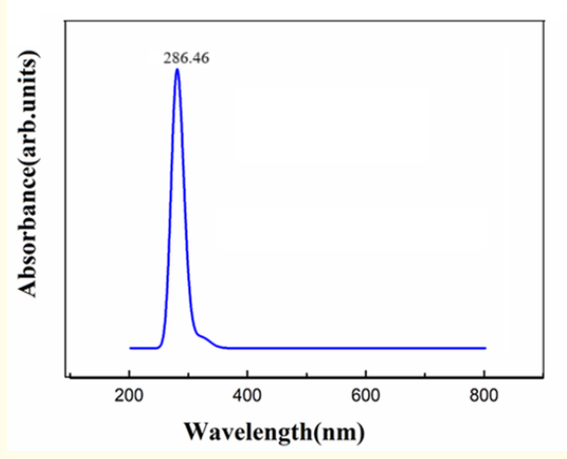

Figure 5: UV visible spectrum of N-Hydroxymethyl phthalimide.

Energy (cm^{-1})	Wavelength (nm)	Osc.Strength	Assignments >10%
31134.61	321.18	0.0001	HOMO->LUMO (96%)
34907.67	286.46	0.0006	H-4->LUMO (19%), H-1->LUMO (72%)
36033.62	277.51	0.0022	H-5->LUMO (45%), H-4->LUMO (27%), H-1->LUMO (21%)

Table 4: Electronic properties of N-hydroxymethyl phthalimide obtained theoretically.

Frontier molecular orbital (FMO)

Global parameters calculated using DFT techniques, presented in Table 5 and Fig.6, describes the wholistic properties of a compound and provides an insight into the stability and also visualises the HOMO- LUMO transitions. FMO offers crucial insights into a charge transfer and molecule's biological activity. Energy difference between Highest Occupied Molecular Orbital (HOMO) and Lowest Unoccupied Molecular Orbital (LOMO) is the energy gap and is a significant parameter in understanding the molecule's stability and reactivity. A smaller HOMO-LUMO gap typically indicates higher reactivity, while a larger gap suggests lower reactivity and hence higher stability. If the absorption peak lies in the UV region, then more amount of energy is required to raise an electron from HOMO to LUMO which indicates that the compound is more stable and less reactive. On contrary, if the absorption peak lies in the visible region, then a lesser amount of energy is sufficient to raise an electron from HOMO to LUMO which indicates that the compound is less stable and highly reactive [39-41]. From the UV graph (ref Fig .5) the title compound's absorption peak lies in the mid UV region indicating that the compound is moderately stable and moderately reactive. A moderately reactive compound may be suitable for biological activity as a compound can be targeted for a specific purpose. From the fig.4 it can be seen that the energy of HOMO and LUMO was found to be -7.743eV and -2.617eV, respectively, which gives an energy gap of 5.126 eV and absorption wavelength of about 242 nm using the equation E = hν. This energy gap obtained from FMO studies compliments the results obtained from UV analysis indicating a moderate stability and reactivity of the title compound. Ionization Potential (IP) is the energy required to remove an electron where IP is associated with HOMO which is the electron donor and IP calculated for title compound was 7.743 eV. LUMO is the electron acceptor in molecular interactions and the energy associated with it is the Electron Affinity (EA), where EA is the energy required to add an electron which is found to be 2.617eV for cho-

sen compound [42]. Electronegativity is the tendency to attract the shared electrons in a chemical bond and for title compound it was found to be 5.180 [42]. Molecules with higher Chemical Hardness (CH) value refers to chemically hard molecules with maximum stability and CH value for N-hydroxymethyl phthalimide was found to be 2.563 which is an indicator of stability and results obtained in UV analysis and HOMO-LUMO energy gap value revels that the title compound is moderately reactive [43]. Softness value presented in Table 5 falls within the desired range which is less than 2 [44] highlighting that the compound is less toxic in nature. Electrophilicity index (EI) is the molecule's ability to accept electrons and EI value calculated is 5.234eV for the title compound. EI value greater than 1.5eV refers to a strong electrophilic nature and thus the title compound has strong electrophilic nature [45, 46] which is also discussed in MEP studies as well. Thus, EI is a descriptor of biological activity of compounds which predicts ability of chosen compound to interact with biological systems by understanding electrophilic nature [47].

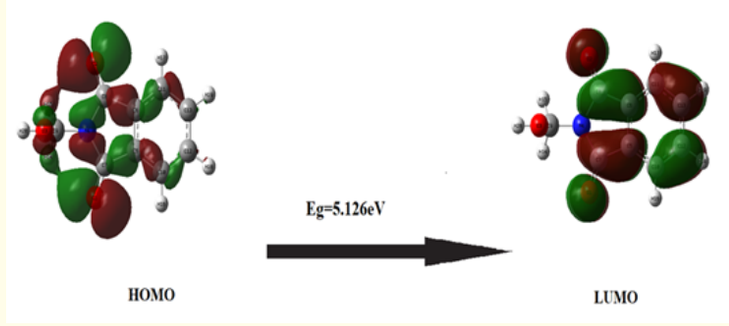

Figure 6: Frontier molecular orbital of N-hydroxymethyl phthalimide.

Global Parameters	Values
HOMO (eV)	-7.743
LUMO (eV)	-2.617
Ionization potential	7.743
Electron affinity	2.617
Energy gap(eV)	5.126
Electronegativity	5.180
Chemical potential	-5.180
Chemical hardness	2.563
Chemical softness	0.195
Electrophilicity index	5.234

Table 5: Calculated energy values N-hydroxymethyl phthalimide.

Biological evaluation

Drug-likeness properties

Drug-likeness properties of N-Hydroxymethyl phthalimide and a standard drug were evaluated using SwissADME online tool and presented in table 6. Adherence to Lipinski's Rule of Five (LRoF) is a critical criterion for identifying potential drug candidates [48]. From Table 6, like the standard drug (Dacarbazine) the title compound meets Lipinski's criteria, with an HBD count of 1, an HBA count of 3, a rotatable bond, and a molecular weight of 177.16g/mol. Lipophilicity is the ability of a molecule to pass through the lipid- based membranes which is a desirable condition for pharmacological applications. The positive value indicates the compound's ability to cross lipid-based membrane indicating a good pharmacokinetic property and a negative value indicates the inability of the compound to pass through the lipid-based membrane. The title compound shows a lipophilicity value +0.72 which is in the desirable range highlighting a good pharmacokinetic property. On contrary, the lipophilicity value of the standard drug is -0.66 predicts its inability to cross the lipid-based membrane. In comparison with the standard drug, title compound exhibits good pharmacokinetic properties [49]. High Gastro-Intestinal (GI) absorption suggests that the chosen compound has good absorption into the gastro-

intestinal and then to bloodstream similar to the standard drug. Blood Brain Barrier is a semi-permeable layer between brain and bloodstream that controls the passage of molecules through it. No BBB permeation predicts that the chosen compound will not enter the brain which is one of the important criteria for a cancer treatment which is complimented by the standard drug values for BBB [50]. The title compound was found to be water-soluble and a good bioavailability score of 0.55 indicates that the chosen compound might be available to biological systems [51,52]. Calculated drug-likeness parameters are within acceptable ranges and which is comparable with the standard drug, Dacarbazine, indicating that N-hydroxymethyl phthalimide possesses favorable properties for drug development towards cancer treatment.

In vitro cytotoxicity activity

N-hydroxymethyl phthalimide was evaluated for its potential toxicity against human skin melanoma (A375) cells. Cells were exposed to different concentrations. To assess cytotoxicity, an MTT assay was performed. Results are given in Table 7. Results revealed cytotoxic effects of title compound on A375 cells. CTC50 value was determined to be 342.13 µg/mL. At 1000 µg/mL, 27% of cells were only viable, and an increased cytotoxic effect on human skin melanoma cell line was observed at higher concentrations [53]. Theoretical analysis, FMO studies, predict that the compound is less toxic in nature.

Ramachandran plot and Molecular docking studies

Ramachandran plots were generated to ensure the stability and reliability of the protein structures. R plots for 1P7K (anti-ssDNA antigen-binding fragment) and 5OTE (MRCK beta in complex with BDP) proteins, which are chosen from protein data bank, are shown in Fig.7. These proteins induce skin melanoma activity. Analysis of the Ramachandran plots revealed that a majority of amino acid residues in both proteins were located within the allowed regions, indicating that the overall protein conformations were stable and favorable for docking studies [54].

Table 6: Drug-likeness parameters for N-hydroxymethyl phthalimide and a standard drug.

Descriptor	Desired range	Values for N-hydroxymethyl phthalimide itle compound)	Values for Dacarbazine (standard drug)
Hydrogen Bond Donors (HBD)	<5	1	2
Hydrogen Bond Acceptors (HBA)	<10	3	4
MlogP	<4.15	0.72	-0.66
molar refractivity	40-130	47.88	44.77
Number of rotatable bonds	<10	1	3
Molecular weight	<500	177.16g/mol	182.18g/mol
GI absorption	-	high	high
Lipinski violation	-	0	0
skin permeation	-	-6.35cm/s	-7.81m/s
Bioavailability score	-	0.55	0.55
BBB permeant	-	No	No
Water solubility	-	soluble	soluble

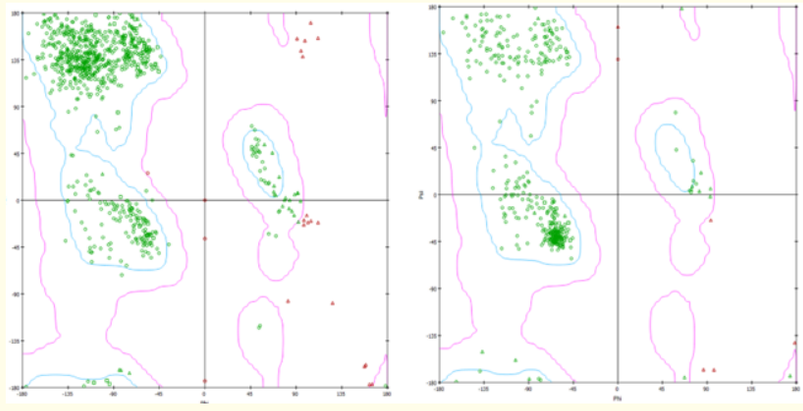

Figure 7: Ramachandran plot of proteins (1P7K and 5OTE).

Concentration of the title compound (µg/mL)	Percentage of A375 cells viable after treatment
1000	27.29 ± 3.35
500	36.54 ± 2.22
250	40.68 ± 4.51
125	44.97 ± 1.41
62.5	60.13 ± 3.74
31.25	77.86 ± 2.33
15.625	88.91 ± 3.15
7.8	96.25 ± 2.21

Table 7: Analysis of the *in vitro* cytotoxicity of N-hydroxymethyl phthalimide against Human Skin Melanoma (A375) cell line by MTT assay.

Molecular docking is a computational method used to study how ligands interact with proteins. It is used to assess the potential therapeutic efficacy of N-hydroxymethyl phthalimide in inhibiting cancer. Anti-metastatic, anti-neoplastic, and anticancer activities of the compound were identified using PASS online tool. Title compound was docked against two skin cancer proteins, 1P7K and 5OTE, using AutoDockTools 1.5.6. Resulting protein-ligand interactions were visualized using Discovery Studio. Fig.8 and Fig.9 provides a visual representation of these interactions in two-dimensions and three-dimensions. Docking result values are presented in Table 8. Binding energies were found to be -4.7kcal/mol and -5.2kcal/mol for 1P7K and 5OTE, respectively. Docking results of standard drug (Dacarbazine) [55] with protein, 5OTE are shown in Fig.10. and binding energy was -3.4 kcal/mol. Binding energy for the chosen compound was greater than commercial drug. Bond parameters provided an insight into the ligand-protein interactions. Shortest bond between O3-H20 atoms was identified in molecular geometry. H20 was bonded with electronegative oxygen (O3) and thus, hydrogen has a partial positive charge which acts as a hydrogen bond donor and is responsible for the protein interaction. Drug-likeness studies identified one HBD and these results are in line with the docking results. Electrophilicity of the chosen compound was identified using FMO studies and electrophilic nature of hydrogen atom (H20) was interpreted in MEP studies incorporates with the docking results. Weakly interacting hydrogen bonds are considered as the driving factor and are significant in maintaining the molecules active and is responsible for the biological reactions. HBD and HBA present in the title compound aids the interaction with biological system through hydrogen bonding. Conventional hydrogen bonding between H20 and the amino acid residue was observed in molecular docking. Conventional hydrogen bonds are also seen between oxygen atoms (O1, O2) and amino acid residues, where oxygen atoms are good hydrogen bond acceptors and three HBA were found in drug-likeness analysis. Results from the dock-

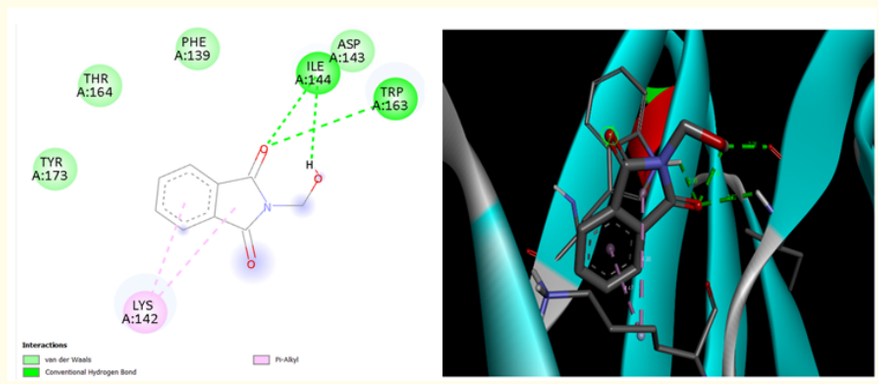

Figure 8: 2D and 3D docking diagram of N-hydroxymethyl phthalimide with 1P7K.

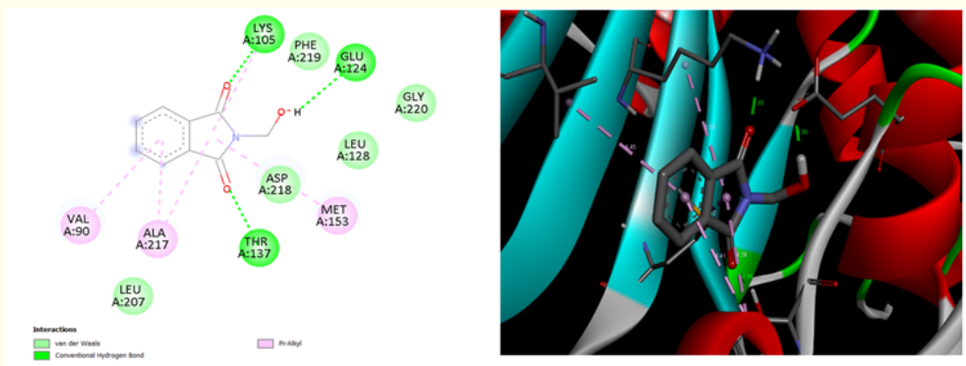

Figure 9: 2D and 3D docking diagram of N-hydroxymethyl phthalimide with 5OTE.

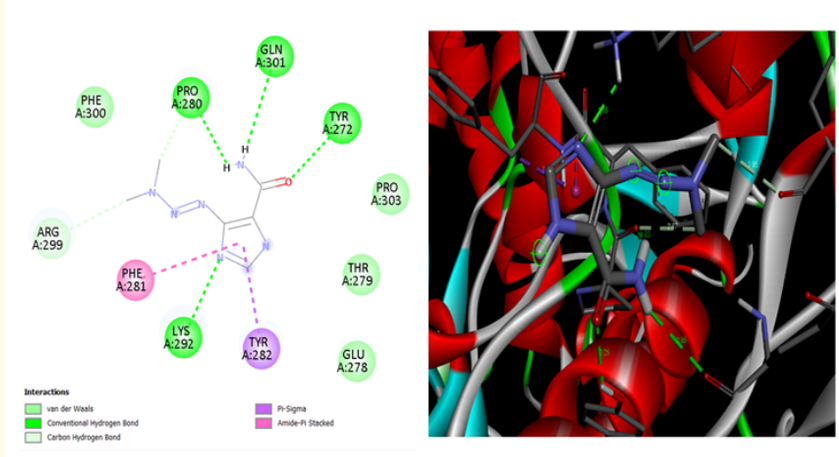

Figure 10: 2D and 3D docking diagram of Dacarbazine with 5OTE.

Table 8: Molecular docking of N-hydroxymethyl phthalimide.

Ligand	Protein	BR	BD(Å)	BE (kcal/mol)	Ref. RMSD	vdw
N-hydroxymethyl phthalimide	1P7K	LEU104	1.988	-4.78	79.66	-5.14
		LYS103	1.929	-4.78	79.6	-5.12
		ILE144	2.121	-4.59	88.05	-5.2
	5OTE	THR137	1.86	-5.2	28.93	-5.48
		PHE219	1.733	-5.2	29.1	-5.46
		LYS105	2.027	-5.15	29.17	-5.4
Commercial drug (Dacarbazine)	5OTE	LEU71	1.77	-3.4	15.41	-4.55
		TYR272	1.925	-3.4	56	-4.47
		PRO280	1.825	-3.37	56.01	-4.42

ing studies fall in line with the other biological parameters studies in the earlier sections of this work predict that N-hydroxymethyl phthalimide exhibits good ligand-protein interaction and thus predicting anti-cancer activity [56,57].

Conclusion

Surface analysis, topological studies and biological evaluation on N-hydroxymethyl phthalimide were carried out using DFT techniques with Gaussian 16W package with Basis set B3LYP 6311++G(d,p). The optimized structure of N-hydroxymethyl phthalimide has been obtained. Molecular geometry of the title compound provided an insight into the structural analysis and biological activity of the molecule. FTIR, FT Raman spectral analyses were carried out and a scaling factor of 0.961 was incorporated in the theoretical values since the experimental and theoretical analysis were done in different phases. Pure O-H stretching peak was observed for title compound, since PED values are 100%, at 3692 cm^{-1} and 3684 cm^{-1} for both experimental and theoretical FT – IR respectively indicating it is an IR active bond. Also, from theoretical and experimental observation pure C-H stretching vibrations were identified at 2963 $cm^{-1}$and 2965 cm^{-1} for FT-IR and FT-Raman respectively. Experimental and theoretical vibrational spectroscopic data of the chosen compound are in line with each other. MEP map provided an insight into the electrophilic attacking sites over oxygen atoms (O2 and O3) and nucleophilic attacking sites over hydrogen atom (H20). Hydrogen atoms (H16, H17, H18, H19) were seen in red region of ELF map indicating the maximum Pauli's repulsion and Carbon atoms (C10, C11) were in blue region indicating minimum Pauli's repulsion. H16, H17, H18, and H19 atoms were seen in the red region of LOL map indicating maximum electron localization and C10 and C11 atoms were in blue region suggesting low electron localization which compliments ELF studies. Surface analysis (MEP, ELF, and LOL maps) predict the possible chemical bonding and interactions, which might play a crucial role in understanding the biological activity of the title compound. Electron interaction

between donors and acceptors were analyzed using NBO. The highest stabilization energy obtained from NBO analysis was 188 kcal/mol, which was observed during the transition of electrons between O2-C8 (donor) and C6-C11 (acceptor). Strong interaction between electron donor and electron acceptor was identified with the higher stabilization energy values obtained in NBO analysis. Absorption peak obtained in UV-Vis analysis suggested the moderate stability and moderate reactivity of the title compound. FMO provided crucial insights into a charge transfer and molecule's biological activity. Calculated energy gap from HOMO-LUMO analysis was found to be 5.126 eV which compliments the UV analysis. From UV analysis and FMO studies predict that the compound is moderately reactive, which may be suitable for biological activity as a compound can be targeted for a specific purpose. Chemical hardness (2.563eV) value suggest that the compound under study is moderately stable. Low chemical softness value (0.172, which is less than 2, indicated the non-toxic nature. Since the Electrophilicity index (5.234) value is greater than 1.5, the title compound exhibits a high electrophilic nature suitable for biological activity. Drug-likeness studies which involve LRoF, BBB, Lipophilicity, GI absorption, water solubility and bioavailability score. These studies were carried out on the title compound and on the standard drug, Dacarbazine, for cancer treatment. Calculated drug-likeness parameters are within acceptable ranges and which is comparable with the standard drug, indicating that N-hydroxymethyl phthalimide possesses favorable properties for drug development towards cancer treatment. An increased cytotoxic effect on human skin melanoma cell line was observed at higher concentrations for the title compound through *in vitro* assay studies. Stability of the skin cancer proteins namely, 1P7K and 5OTE, was analyzed using Ramachandran plot and it was found suitable for docking with the chosen ligand. Molecular docking studies between the chosen proteins, 1P7K and 5OTE, and the ligand were carried out and the binding energies were found to be -4.7 kcal/mol, and -5.2 kcal/mol respectively. Binding energy of the title compound was found to be greater than the standard drug which is -3.4kcal/mol. Results from the docking studies fall in line with the other biological parameters studied, in this work, predict that N-hydroxymethyl phthalimide exhibits good ligand-protein interaction and thus predicting anticancer activity to inhibit skin melanoma.

Bibliography

1. Kushwaha N and Kaushik D. "Recent advances and future prospects of phthalimide derivatives". *Journal of Applied Pharmaceutical Science* 6.3 (2016): 159-171.
2. Jamel NM., *et al*. "Methods of Synthesis Phthalimide Derivatives and Biological Activity-Review". *Journal of Pharmaceutical Sciences and Research* 11.9 (2019): 3348-3354.
3. Fernandes GF., *et al*. "Phthalimide as a versatile pharmacophore scaffold: Unlocking its diverse biological activities". *Drug Development Research* 84.7 (2023): 1346-1375.
4. Matore BW., *et al*. "Phthalimides Represent a Promising Scaffold for Multi-Targeted Anticancer Agents". *Chemistry Select* 8.9 (2023): e202204851.
5. Asadollahi A., *et al*. "Synthesis, molecular docking, and antiepileptic activity of novel phthalimide derivatives bearing amino acid conjugated anilines". *Research in Pharmaceutical Sciences* 14.6 (2019): 534-543.
6. F Lamie P., *et al*. "Design, synthesis and evaluation of novel phthalimide derivatives as *in vitro* anti-microbial, anti-oxidant and anti-inflammatory agents". *Molecules* 20.9 (2000): 16620-16642.
7. Frisch MJ., *et al*. "Gaussian16 Revision A. 03 (Wallingford, CT: Gaussian Inc.) (2016).
8. Dennington Roy., *et al*. "GaussView, Version (2009).
9. Jamróz MH. "Vibrational Energy Distribution Analysis; VEDA 4 Program, Warsaw, Poland". 2004–2010.
10. Lu T and Chen F. "Multiwfn: A multifunctional wavefunction analyzer". *Journal of Computational Chemistry* 33.5 (2012): 580-592.
11. Antoine Daina. "Swiss ADME: a free web tool to evaluate pharmacokinetics, drug-likeness and medicinal chemistry friendliness of small molecules". *Scientific Reports* 7 (2017): 42717.
12. Filimonov DA., *et al*. "Prediction of the biological activity spectra of organic compounds using the PASS online web resource". *Chemistry of Heterocyclic Compounds* 50 (2014): 444-457.
13. R Huey., *et al*. "Using AutoDock 4 and AutoDock vina with AutoDockTools: a tutorial, The Scripps Research Institute Molecular Graphics Laboratory 10550.92037 (2012): 1000.
14. Dassault Systemes BIOVIA: Discovery Studio Visualizer (2000): 21.1.0.20298.
15. Prasana Johanan., *et al*. "Wavefunction analysis, charge transfer and molecular docking studies on famciclovir and entecavir: Potential anti-viral drugs". *Chemical Data Collections* 26 (2020): 100353.

16. Jebapriya J Christina., *et al*. "Crystal structure, synthesis, growth and characterization of a non-linear chalcone crystal: (2E)-1- (4-chlorophenyl)-3- (4-diethylaminophenyl)-prop-2-en-1-one". *Journal of Molecular Structure* 1246 (2021): 131184.

17. Priscilla J., *et al*. "Experimental and theoretical spectroscopic analysis, hydrogen bonding, reduced density gradient and antibacterial activity study on 2-Phenyl quinoline alkaloid". *Chemical Physics* 536 (2020): 110827.

18. Clara TH., *et al*. "Structural, optical, thermal, dielectric and Z-scan study on novel (2E)-1- (4-aminophenyl)-3-(4-benzyloxyphenyl)-prop-2-en-1-one (APBPP) chalcone crystal for nonlinear optical applications". *Optical Materials* 109 (2020): 110331.

19. Jomaa I., *et al*. "Insight into non-covalent interactions in a tetrachlorocadmate salt with promising NLO properties: experimental and computational analysis". *Journal of Molecular Structure* 1242 (2021): 130730.

20. Anju LS., *et al*. "Spectroscopic, quantum mechanical and docking studies on organochlorine insecticides by density functional theory". *Journal of Molecular Structure* 1208 (2020): 127904.

21. Michalska D., *et al*. "Density functional, Hartree– Fock, and MP2 studies on the vibrational spectrum of phenol". *The Journal of Physical Chemistry* 100.45 (1996): 17786-17790.

22. Tanak H and Marchewka MK. "FT-IR, FT-Raman, and DFT computational studies of melaminium nitrate molecular–ionic crystal". *Journal of Molecular Structure* 1034 (2013): 363-373.

23. Edwin B and Joe IH. "Vibrational spectral analysis of anti-neurodegenerative drug Levodopa: A DFT study". *Journal of Molecular Structure* 1034 (2013): 119-127.v

24. Barnes AJ., *et al*. "The resonance Raman spectra of Orange II and Para Red: molecular structure and vibrational assignment". *Spectrochimica Acta Part A: Molecular Spectroscopy* 41.4 (1985): 629-635.

25. Saji Rinnu Sara., *et al*. "Experimental and theoretical spectroscopic (FT-IR, FT-Raman, UV-VIS) analysis, natural bonding orbitals and molecular docking studies on 2-bromo-6-methoxynaphthalene: A potential anti-cancer drug". *Heliyon* 7.6 (2021).

26. Aswathy P., *et al*. "Enhanced NLO response and switching self-focussing in benzodiazepine derivative with–NO2 and-Br substitution". *Heliyon* 9.10 (2023).

27. Gadre SR., *et al*. "Molecular electrostatic potentials: A topographical study". *The Journal of Chemical Physics* 96.7 (1992): 5253-5260.

28. Gopi B and Vijayakumar V. "Synthesis and molecular docking of novel indazole derivatives with DFT studies" (2024).

29. Arthur DE and Uzairu A. "Molecular docking studies on the interaction of NCI anticancer analogues with human Phosphatidylinositol 4, 5-bisphosphate 3-kinase catalytic subunit". *Journal of King Saud University-Science* 31.4 (2019): 1151-1166.

30. Tarika JDD., *et al*. "Tuning the Computational Evaluation of Spectroscopic, ELF, LOL, NCI analysis and Molecular Docking of Novel Anti COVID-19 Molecule 4-Dimethylamino Pyridinium 3, 5-Dichlorosalicylate". *Spectrochimica Acta, Part A: Molecular and Biomolecular Spectroscopy* 259 (2021): 119907.

31. Abraham CS., *et al*. "Quantum computational studies, spectroscopic (FT-IR, FT-Raman and UV–Vis) profiling, natural hybrid orbital and molecular docking analysis on 2, 4 Dibromoaniline". *Journal of Molecular Structure* 1160 (2018): 393-405.

32. Sangeetha P., *et al*. "Spectroscopic analysis of 2-amino-1-naphthalenesulfonic acid, molecular docking, and evaluation of the electronic properties of several solvents". *Spectroscopy Letters* 56.6 (2023): 323-342.

33. Akman F., *et al*. "Molecular Structure, Electronic Properties, Reactivity (ELF, LOL, and Fukui), and NCI-RDG Studies of the Binary Mixture of Water and Essential Oil of *Phlomis bruguieri"*. Molecules 28.6 (2023): 2684.

34. S Pallen., *et al*. "Advances in nonlinear optical microscopy techniques for *in vivo* and *in vitro* neuro-imaging". *Biophysical Reviews* 13 (2021): 1199–1217.

35. Gangadharan R and Sampath Krishnan S. "Natural Bond Orbital (NBO) population analysis of 1-azanapthalene-8-ol". *Acta Physica Polonica A* 125.1 (2014): 18-22.

36. Madhavan VS., *et al*. "Natural Bond Orbital (NBO) Analysis of Certain Salicylanilide Derivatives".

37. Hemachandran K., *et al*. "Structural activity analysis, spectroscopic investigation, biological and chemical properties interpretation on Beta Carboline using quantum computational methods". *Heliyon* 5.11 (2019).

38. Fathima Rizwana B., *et al*. "Spectroscopic investigation (FT-IR, FT-Raman, UV, NMR), Computational analysis (DFT method) and Molecular docking studies on 2- (acetyloxy) methyl. -4-(2-amino-9h-purin-9-yl) butyl acetate". *International Journal of Materials Science* 12 (2017): 196-210.

39. J Rezvan Vahideh Hadigheh. "Molecular structure, HOMO–LUMO, and NLO studies of some quinoxaline 1, 4-dioxide derivatives: Computational (HF and DFT) analysis". *Results in Chemistry* 7 (2024): 101437.

40. Rastogi VK., *et al*. "FTIR and FT-Raman spectra and density functional computations of the vibrational spectra, molecular geometry and atomic charges of the biomolecule: 5-bromouracil". *Journal of Raman Spectroscopy: An International Journal for Original Work in all Aspects of Raman Spectroscopy, Including Higher Order Processes, and also Brillouin and Rayleigh Scattering* 38.10 (2007): 1227-1241.

41. Amalanathan M., *et al*. "FT-IR and FT-Raman spectral investigation and DFT computations of pharmaceutical important molecule: ethyl 2- (4-Benzoyl-2, 5-dimethylphenoxy) acetate. *Pharm Anal Acta* 7.457 (2016): 26-28.

42. Miar Marzieh., *et al*. "Theoretical investigations on the HOMO–LUMO gap and global reactivity descriptor studies, natural bond orbital, and nucleus-independent chemical shifts analyses of 3-phenylbenzo d. thiazole-2 (3 H)-imine and its para-substituted derivatives: Solvent and substituent effects". *Journal of Chemical Research* 45.1-2 (2021): 147-158.

43. Pearson Ralph G. "Chemical hardness and density functional theory". *Journal of Chemical Sciences* 117 (2005): 369-377.

44. Manjusha P., *et al*. "A computational and spectroscopic interpretation (FT-IR, FT-Raman, UV–vis and NMR) with molecular docking studies on 3-carboxy-2-hydroxy-N, N, N-trimethyl-1-propanaminium hydroxide: A pharmaceutical drug". *Chemical Data Collections* 20 (2019): 100191.

45. Rijal., *et al*. "Molecular simulation, vibrational spectroscopy and global reactivity descriptors of pseudoephedrine molecule in different phases and states". *Heliyon* 9.3 (2023).

46. Kumer A., *et al*. "The simulating study of HOMO, LUMO, thermo physical and quantitative structure of activity relationship (QSAR) of some anticancer active ionic liquids". *Eurasian Journal of Environmental Research* 3.1 (2023): 1-10.

47. Magdaline JD and Chithambarathanu T. "Vibrational spectra (FT-IR, FT-Raman), NBO and HOMO, LUMO studies of 2-thiophene carboxylic acid based on density functional method". *IOSR Journal of Applied Chemistry* 8 (2015): 6-14.

48. Lipinski CA. "Lead-and drug-like compounds: the rule-of-five revolution". *Drug Discovery Today: Technologies* 1.4 (2004): 337-341.

49. Chandrasekaran Balakumar., *et al*. "Computer-aided prediction of pharmacokinetic (ADMET) properties". *Dosage form design parameters*. Academic Press (2018): 731-755.

50. Gawdi Rohin and Prabhu Emmady. "Physiology, blood brain barrier". *StatPearls* (2020).

51. Narvekar Mayuri., *et al*. "Nanocarrier for poorly water-soluble anticancer drugs-barriers of translation and solutions". *Aaps Pharmscitech* 15 (2014): 822-833.

52. Price G and Patel DA. "Drug bioavailability" (2020).

53. Denizot F and Lang R. "Rapid colorimetric assay for cell growth and survival: modifications to the tetrazolium dye procedure giving improved sensitivity and reliability". *Journal of Immunological Methods* 89.2 (1986): 271-277.

54. Thomas R., *et al*. "Two neoteric pyrazole compounds as potential anti-cancer agents: synthesis, electronic structure, physico-chemical properties and docking analysis". *Journal of Molecular Structure* 1181 (2019): 455-466.

55. Eggermont Alexander MM and John M Kirkwood. "Re-evaluating the role of dacarbazine in metastatic melanoma: what have we learned in 30 years". *European Journal of Cancer* 40.12 (2004): 1825-1836.

56. Manimegalai P., *et al*. "*In-vitro* antibacterial, antioxidant and anti-inflammatory and In-silico ADMET, molecular docking study on Hardwickia binata phytocompunds with potential inhibitor of skin cancer protein". *In Silico Pharmacology* 11.1 (2023): 25.

57. Umar AB., *et al*. "Molecular docking strategy to design novel V600E-BRAF kinase inhibitors with prediction of their drug-likeness and pharmacokinetics ADMET properties". *Chemistry Africa* 4.31 (2021): 189-205.